

Resonant photoemission study of the electronic structure of CuO and Cu₂O

J. Ghijsen,* L. H. Tjeng, H. Eskes, and G. A. Sawatzky

Department of Solid State and Applied Physics, Material Research Centre, University of Groningen, Nijenborgh 18, NL-9747 AG Groningen, The Netherlands

R. L. Johnson

Universität Hamburg, II. Institut für Experimentalphysik, Laruper Chaussee 149, D-2000 Hamburg 50, Federal Republic of Germany

(Received 7 December 1989)

The electronic structures of CuO and Cu₂O have been investigated by resonant photoemission at the copper 3*p* threshold. The experimental data from CuO are compared with the results of a cluster calculation. From this analysis we confirm the dominant *d*⁸ character of the states between 8 and 16 eV, and that singlet and triplet final states behave quite differently at the (3*p*→3*d*) resonance. It is necessary to specify the multiplet state when calculating the *d*-*d* Coulomb interaction in this case since the total energy spread of the *d*⁸ multiplets is about 8 eV. The results confirm the charge-transfer nature of the band gap in CuO. The resonance behavior in Cu₂O is explained in terms of strong O 2*p*-Cu 4(*sp*) hybridization.

I. INTRODUCTION

In a previous article,¹ we reported on an investigation of the electronic structure of CuO and Cu₂O by x-ray and ultraviolet photoemission (XPS and UPS), inverse photoemission [bremsstrahlung isochromat spectroscopy (BIS)], and Auger electron (AES) spectroscopies. It was found that whenever the final state has no more than one hole in the copper *d* shell the description provided by one-electron band theory² is adequate. On the other hand, situations involving more than one hole in the *d* shell are better described using a configuration-interaction (CI) model.³ Electron-correlation effects are thus found to be important in Auger spectra of both materials and in photoemission spectra from CuO, whereas photoemission results from Cu₂O as well as inverse photoemission results from both materials can be described by one-electron band theory. The relative size of the Coulomb energy $U(3d, 3d)$ and of the charge-transfer energy Δ found in CuO make it a charge-transfer semiconductor, corresponding to class *B* of the Zaanen-Sawatzky-Allen (ZSA) diagram.⁴ These compounds are also good model compounds for obtaining model Hamiltonian parameters for the high- T_c superconductors as we have discussed in recent reviews.⁵⁻⁸

As a confirmation of our previous results,¹ and to gain a better understanding of the electronic structure of these materials, we use in this work resonant photoemission spectroscopy (RPES). This technique has now become a standard tool for investigating the electronic structure of a wide range of materials: transition metals,⁹⁻¹¹ rare earth,^{12,13} actinide¹³ compounds, and high- T_c superconducting oxides.¹⁴ The resonance of interest in the present case is at the copper 3*p* threshold for photon energies around 74 eV.

Resonant photoemission on Cu, Cu₂O, and CuO has al-

ready been reported by Thuler *et al.*¹¹ whose experimental data are consistent with ours, but have somewhat lower resolution. Our aim is to obtain a more quantitative description of the resonance process. It can be expected that triplet final states resonate less strongly than singlet states. Indeed, the simplest description of resonant photoemission in CuO would allow only singlet states to resonate.¹⁵ A more complete approach was used by Okada and Kotani¹⁶ who did, however, neglect the multiplet structure. Furthermore, the location of resonating peaks will provide conclusive information about the *d*⁸ character of the final states involved and the total energy spread of the different multiplets.

II. EXPERIMENTAL SETUP AND SAMPLE PREPARATION

High-purity copper foils were oxidized according to the procedure described in Ref. 1. The cleanliness of the samples was also checked by XPS. In order to fix the energy scale, we recorded the Fermi edge of clean copper for a set of selected photon energies. This Fermi energy was chosen as the zero point of the binding energy scale. The stability of the oxide film upon exposure to synchrotron light was checked by duplicating some spectra, but no changes were observed.

The measurements were performed at the Flipper II beam line at the storage ring Doris at Hasylab. The experimental setup has been described elsewhere.¹⁷ The base pressure was better than 10⁻¹⁰ mbar. The data were collected in the angle-integrating mode using a double pass cylindrical mirror analyzer. The analyzer and monochromator resolution in the vicinity of the Cu 3*p* resonance are 0.30 eV (FWHM) each for the settings we used in this experiment.

III. CuO

A. Theory

The model Hamiltonian³ used describes a CuO₄⁶⁻ cluster in D_{4h} symmetry which corresponds quite well to the local symmetry of copper in CuO.¹⁸ We take into account the Coulomb interaction between copper 3d states, but neglect it within the oxygen 2p shell, as well as between O 2p and Cu 3d states:

$$H = H_0 + H_1 ,$$

$$H_0 = \sum_m \varepsilon_d(m) d_m^\dagger d_m + \sum_m \varepsilon_p(m) p_m^\dagger p_m \quad (1)$$

$$+ \sum_m T_{pd}(m) (p_m^\dagger d_m + d_m^\dagger p_m) ,$$

$$H_1 = \sum_{m,m',n,n'} U(m,m',n,n') d_m^\dagger d_m d_n^\dagger d_n ,$$

where H_0 is the one-particle Hamiltonian. d^\dagger (p^\dagger) operator creates a hole with energy ε_d (ε_p) in the Cu 3d (O 2p) shell. The third term of H_0 describes the Cu 3d–O 2p hybridization. H_1 describes the Coulomb interaction within the Cu 3d shell. The subscripts stand for the orbital and spin quantum numbers identifying the various states in the irreducible representations of the D_{4h} point group. $\varepsilon_p(m)$ includes the interatomic oxygen-oxygen interaction T_{pp} , which is a quarter of the total oxygen band width. $U(m,m',n,n')$ can be expressed in terms of the Racah A , B , and C parameters. We neglect the point charge contribution to the total ligand field,¹⁹ so that $\varepsilon_d(m) \equiv \varepsilon_d$ is symmetry independent. The values we use for the energy parameters are listed in Table I. This Hamiltonian is solved under the further assumption that orbitals centered on different atoms are orthogonal (i.e., neglecting overlap can be compensated by the use of effective parameters). It describes rather well the contribution of the orbitals from the central copper atom, but perhaps less accurately the contribution of the oxygen atoms on the corners. We consider only those combinations of O 2p orbitals with the same symmetry as the copper d orbitals, viz. a_{1g} ($3z^2 - r^2$), b_{1g} ($x^2 - y^2$), b_{2g} (xy), and e_g (xz, yz). The applicability of our calculations is thus restricted to the photon energy domain where the photoionization cross section is much smaller for O 2p levels than for Cu 3d. This is certainly the case

TABLE I. Parameters used in the CuO₄ cluster Hamiltonian.

m	$\varepsilon_d(m)$	$\varepsilon_p(m)$	$t_{pd}(m)$
a_{1g}	0	$\Delta + T_{pp}$	$t_{pd}(b_{1g})/\sqrt{3}$
b_{1g}	0	$\Delta - T_{pp}$	$t_{pd}(b_{1g})$
b_{2g}	0	$\Delta + T_{pp}$	$t_{pd}(b_{1g})/2$
e_g	0	Δ	$t_{pd}(b_{1g})/2\sqrt{2}$
Δ	= 2.75 eV		$A = 6.5$ eV
$T_{pd}(b_{1g})$	= 2.5 eV		$B = 0.15$ eV
T_{pp}	= 1.0 eV		$C = 0.58$ eV

of XPS,²⁰ remains qualitatively true for as low a photon energy as 40.8 eV (He II), but is no longer valid at a photon energy of 21.2 eV (He I).¹ It can thus be expected to hold for a photon energy at the Cu ($3p \rightarrow 3d$) absorption threshold.

The $M_{2,3}M_{4,5}M_{4,5}$ Auger-type interaction as well as the interaction with the electromagnetic field are treated as perturbations:

$$V = V_{3p-3d} + D ,$$

$$V_{3p-3d} = \sum_{h,i,j,k} U(h,i,j,k) d_h^\dagger d_i^\dagger c_j e_k + \text{H.c.} , \quad (2)$$

$$D = \sum_{i,j} D_{pd}(i,j) c_i^\dagger d_j + \sum_{i,j} D_{d,e}(i,j) d_i^\dagger e_j + \text{H.c.} ,$$

where c_j^\dagger creates a hole in the Cu 3p shell and e_k^\dagger creates a vacancy for the outgoing electron. The only nonzero terms in V_{3p-3d} are those for which the outgoing electron has p, f or h symmetry ($l = 1, 3$, or 5 , Ref. 21). D is treated within the dipole approximation. The probability of a transition from the ground state g to a two-hole final state f with emission of an outgoing electron e_l is then given by

$$P_{g \rightarrow f} = |\langle f | V + V(E - H + i\Gamma)^{-1} V + \dots | g, e_l \rangle|^2 , \quad (3)$$

where the first and second term represent the direct and indirect photoemission process, respectively. The interference of these processes leads to a Fano resonance^{22,23} when the photon energy is varied around the binding energy of the Cu 3p level. The intensity collected for a particular photon energy $h\nu$ is proportional to

$$I(h\nu, f, e_l) = |\langle f | D | g, e_l \rangle + \sum [\langle f | V_{3p-3d} | j_{3p} j'_{e_l} JM \rangle \langle j_{3p} j'_{e_l} JM | D | g, e_l \rangle / (\Delta E_j + i\Gamma_j)]|^2 \quad (4)$$

with

$$\Delta E_j = h\nu - E_b(3p_j) \quad (5)$$

The summation extends over all intermediate states $|j_{3p} j'_{e_l} JM\rangle$, that describe a vacancy in the Cu 3p shell jj coupled with the vacancy of the outgoing electron. The half-width Γ_j of the intermediate state is given by

$$\Gamma_j = \pi\rho \sum |\langle f | V | j_{3p} j'_{e_l} JM \rangle|^2 / (2j+1) , \quad (6)$$

where ρ is the density of states of the continuum and the summation extends over f, j', J , and M . Despite the high degree of polarization of synchrotron light, relation (4) has to be averaged over all orientations, because we use polycrystalline samples.

Although the angular part of the matrix elements involved in relation (4) is independent of any assumption on the wave functions involved, this is not the case for the radial part. The radial part of the Auger matrix elements have been computed by McGuire²⁴ from the wave functions of Herman and Skillman (HS).²⁵ The radial parts of the absorption matrix elements have been computed by Davis and Feldkamp,²⁶ who use also HS wave functions. Numerical values are displayed in Table II.

The values of the matrix elements of r we use in our calculation differ from those used by Davis and Feldkamp.^{26,27} They found that for transition metals, from Cr to Ni, a value for 2.5 for $\langle 3d|r|e_f \rangle / \langle 3p|r|3d \rangle$ was adequate. In order to obtain enough on-resonance intensity for the mostly Cu d^8 and d^{10} levels (at binding energies between 8 and 16 eV), we had to reduce the ratio to unity (Table II). In order to limit the number of parameters, we keep the value of Ref. 25 for the ratio $\langle 3d|r|e_p \rangle / \langle 3d|r|e_f \rangle$. As discussed in the following, the intensities found for an outgoing p electron are expected to be very small, and it is not possible to derive the corresponding matrix elements of r from a comparison with the experiment. The Coulomb matrix elements from Ref. 24 have been divided by $\sqrt{2}$, since it has been observed that McGuire's matrix elements are too large by that amount.²⁷⁻²⁹ Using relation (6), one gets 0.84 eV for the half width of both $3p_{1/2}$ and $3p_{3/2}$ levels, in good agreement with the experimental values of 1.0 and 0.8 eV. Such a comparison makes sense because the width of those levels is mainly due to super-Coster-Kronig transitions.^{28,30} The $R^k(3d,3d;3p,e_h)$ matrix elements (involving an outgoing h electron) were neglected because they are quite small. Although the Coulomb matrix elements involving an outgoing p electron are about three times larger,²⁴ the corresponding intensity is still rather small compared to that from f emission. Only in the case of a $^1A_{1g}$ final state (small peak at a binding energy of about 16 eV) are the interference effects for an outgoing p electron found to be comparable with those for an f electron, but that resonance is extremely weak. Nonetheless, they were included in our calculation.

A more likely source of discrepancy is the neglect of the resonance channel that goes through the temporary promotion of a Cu $3p$ electron to the $4s$ shell. In atomic copper, $\langle 3p|r|4s \rangle$ is smaller than, but comparable to $\langle 3p|r|3d \rangle$.²⁶ The magnitude of the $R^k(3d,4s;3p,e_l)$ in-

tegrals lies between that of $R^k(3d,3d;3p,e_p)$ and $R^k(3d,3d;3p,e_f)$.²⁴ Although it is conceivable to treat $(3p \rightarrow 4s)$ resonances in the same way as the $(3p \rightarrow 3d)$ process, it is questionable whether a cluster calculation is well adapted to the description of states involving contributions from the Cu $4s$ shell (even with effective parameters), because of their diffuse, delocalized nature.

B. Results and discussion

Figure 1 displays valence-band spectra measured in the vicinity of the Cu $3p$ resonance. The data have been corrected for the analyzer transmission, which was taken proportional to the reciprocal kinetic energy. The inelastic background was subtracted from valence-band spectra under the assumption that its intensity at a given energy is proportional to the peak area between that energy and the Fermi level. Measured and computed spectra on and off resonance, at the Cu $3p_{3/2}$ threshold, are compared in Fig. 2. Although the agreement between theory and experiment is not perfect, one does see strong similarities. Important points to note are the following: Clearly the dominant d^8 character lies at energies above 8 eV, the singlet states resonate much more than do the triplets, and the resonant behavior up to about 8 eV is very small.

It appears that the binding energies obtained from the cluster calculation agree reasonably well with those found experimentally, except that the spread of the mostly d^8 levels (from 8 to 16 eV) is about 1 eV too large. This can be improved by using a larger cluster or an Anderson impurity model.³

The discrepancies observed for the intensities may be due to several causes. First, photoemission from the oxygen site was completely neglected in view of the difference of cross section of Cu $3d$ and O $2p$ shells.²⁰ Note that to improve this point, it is not sufficient to add up copper and oxygen intensities, but that a possible interference effect has to be considered.³¹ Second, the results of our cluster calculation were uniformly broadened by 1 eV. A broadening proportional to the square of the binding energy would be more realistic, but makes little sense if the oxygen contribution is not included in the first place. Finally, there are arguments pointing towards different magnitudes for the transfer integrals: $\langle d^{10}\underline{L}^2|H|d^9\underline{L} \rangle = t_{pd}(10)$ and $\langle d^9\underline{L}|H|d^8 \rangle = t_{pd}(8)$,³²⁻³⁴ where \underline{L} denotes a hole in the outer shell of

TABLE II. Numerical values used to compute photoemission spectra of CuO near the Cu $3p$ resonance, compared with some values from the literature.

	This work	Literature	Reference
$R^1(3d,3d;3p,e_f)$	-2.04 eV	-2.89 eV	23
$R^3(3d,3d;3p,e_f)$	-1.01 eV	-1.43 eV	23
$R^1(3d,3d;3p,e_p)$	0.38 eV	0.54 eV	23
$R^3(3d,3d;3p,e_p)$	0.38 eV	0.54 eV	23
ρ	0.0735 eV ⁻¹	0.0735 eV ⁻¹	23
$\Delta_{s-o}(\text{Cu } 3p)$	2.2 eV	2.2 eV	11
$\langle 3d r e_f \rangle / \langle 3p r 3d \rangle$	1	2.5	25,26
$\langle 3d r e_p \rangle / \langle 3p r 3d \rangle$	0.2	0.49	25,26

the ligand. This last point we discuss in more detail in the following.

In the case of nickel dihalides, it appears that $T_{pd}(n+1)$ is smaller than $T_{pd}(n-1)$ with $n=9$ (Ref. 32). Gunnarsson *et al.*³³ found that the opposite holds for $\text{Cd}_{1-x}\text{Mn}_x\text{Te}$ and leads to good agreement with experimental results obtained from resonant photoemission.⁹ Two opposing effects are involved: The additional e/r term due to one more hole in the transition-metal ion tends to increase the $t_{pd}(n-1)$ relative to $t_{pd}(n+1)$, whereas the associated contraction of the d shell has the opposite effect. The first effect seems to dominate in ionic compounds, the latter in more covalent materials.³⁴ In Fig. 3 we display the results obtained when either $tpd(8)$ or $tpd(10)$ has been multiplied by a factor of 1.2. Besides the change this produces on the binding energies, varying the t_{pd} matrix elements mainly affects the relative intensities of the peaks around 9.5 and 12 eV binding energy. The experimental results are better reproduced when $t_{pd}(8)$ is larger than $t_{pd}(10)$.

In Fig. 4(a) we display the constant-initial-state (CIS)

spectrum measured at a binding energy of 12 eV and compare it to the corresponding calculated spectrum. This particular binding energy was chosen because it shows the largest resonance effect. The data have been corrected for the monochromator and analyzer transmission but not for the inelastic background, so the superimposed curves do not have the same zero point on the y axis. The slope of the asymptote to the measured spectrum reflects the variation of the photoionization cross section with photon energy.²⁰ This effect is absent from the calculated curve because we use photon-energy independent matrix elements. Nevertheless, a comparison of the two curves allows us to check that the spin-orbit splitting of the Cu $3p$ levels corresponds well to the separation of the two CIS peaks. Also, the relative intensities of these two peaks are well reproduced by our calculation. Furthermore, it is important to note that the tail of the CIS profile is on the high proton energy side, because this confirms the sign of the ratio $\langle 3d|r|e_f \rangle / \langle 3p|r|3d \rangle$. In Fig. 4(b) we display CIS curves calculated for different binding energies. The low binding energy peaks have

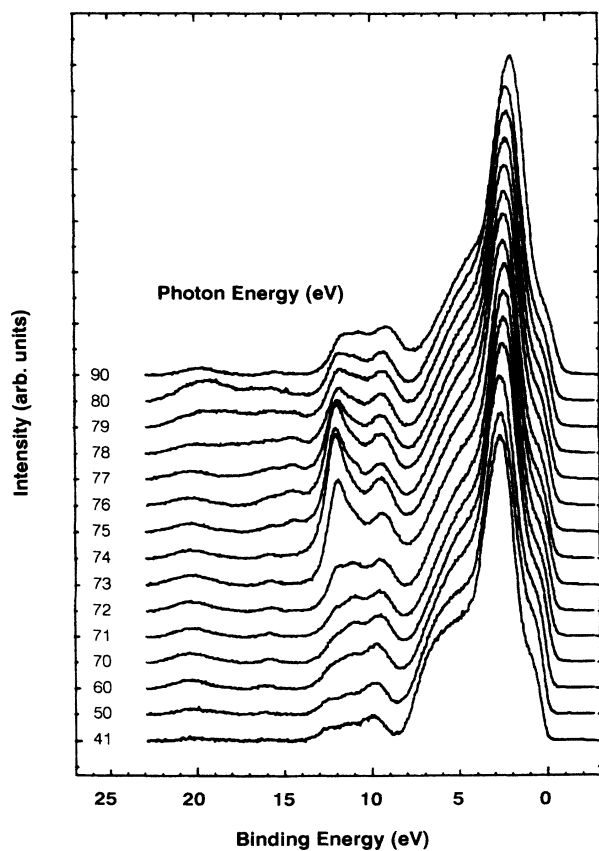


FIG. 1. Valence-band spectra of CuO recorded around the copper $3p$ threshold. The correction for the analyzer transmission and the background removal procedure are explained in the text.

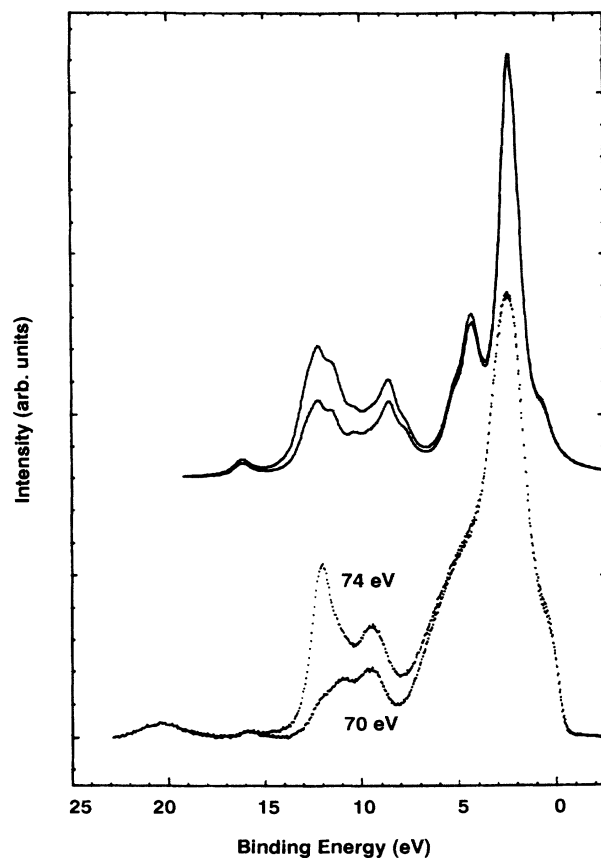


FIG. 2. Valence-band spectra of CuO recorded at photon energies of 74 and 70 eV, compared with intensities calculated at the Cu $3p_{3/2}$ threshold and 4 eV below. The results of the cluster calculation have been Lorentz broadened by 1 eV.

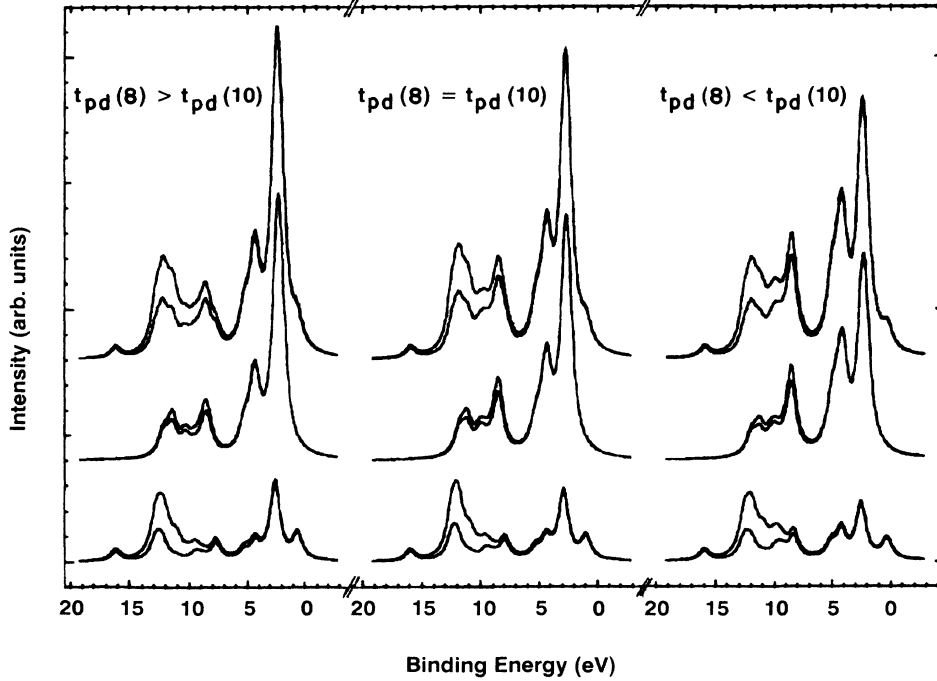


FIG. 3. Valence-band spectra of CuO calculated for different values of $t_{pd}(8)$ and $t_{pd}(10)$; the resonance of singlet states (bottom) and triplet states (middle) have been drawn together with the full spectrum (top). Left: $t_{pd}(8)$ enhanced by 20%, center: $t_{pd}(8)=t_{pd}(10)$, right: $t_{pd}(10)$ enhanced by 20%.

such small resonances that it is difficult to obtain accurate CIS plots, especially because of the Ni coating of the monochromator.¹⁷ A detailed comparison with theory is therefore difficult. Nevertheless, it is worth noting that the lowest binding energy peak which we have previously interpreted as a singlet bound state³⁵ and which corresponds to the singlet described by Zhang and Rice³⁶ shows only a weak antiresonance that confirms its dominant $d^9\bar{L}$ and $d^{10}\underline{L}^2$ character.

IV. Cu₂O

Cu₂O is known to have a formally full $3d$ band,¹ therefore $3d^8$ final states should not be visible in the one-electron removal spectrum, unless the final state is in fact $3d^8 4(sp)^1$. This state can be reached because the ground state of Cu₂O hybridizes $3d$ and $4(sp)$ shells:

$$|g\rangle = \alpha|3d^{10}\rangle + \beta|3d^9 4(sp)^1\rangle + \gamma|3d^{10}\underline{L} 4(sp)^1\rangle \quad (7)$$

Such a mixing occurs because the Cu $4(sp)$ and $3d(3z^2-r^2)$ orbitals both combine with the O $2p_z$ orbitals of the neighboring oxygen atoms, and because the local surrounding of the copper has a low symmetry. The intermediate state in RPES would be $3p^5 3d^{10} 4(sp)$ (Ref. 1) whose optical oscillator strength will be determined by β^2 in Eq. (7). This together with the fact that the resonating final state is essentially $3d^8 4(sp)$ (Ref. 1) has a very straightforward consequence: The photon energy at the resonance is larger than in CuO because some extra energy is needed to excite a $3d$ electron to the $4(sp)$ shell.

Similarly, the final state that resonates most has a higher binding energy in Cu₂O than in CuO. For the same reason as in CuO, it is doubtful that a $(3p \rightarrow 4s)$ resonant process can be adequately described in terms of atomic matrix elements. Igarashi^{37,38} has calculated resonant photoemission intensities for copper halides, solving exactly the three-body problem involving two valence holes and an optically excited conduction electron [$3d^8 4(sp)$ (Ref. 1) final state]. However, Ishii *et al.*¹⁰ found that the spectra of copper halides are quite different from that of Cu₂O. This is perhaps partially due to differences in data evaluation, but the local symmetry around copper atoms has also to be considered. Therefore we discuss our results by comparison with data collected on Ag₂O (Ref. 39). The instability of AgO in vacuo precludes a similar comparison being performed with CuO.

Valence-band spectra measured at photon energies around the Cu $3p$ photoionization threshold are shown in Fig. 5. Most of the resonant enhancement occurs at binding energies around 15.3 eV. These states are thus predominantly $3d^8 4(sp)$ (Ref. 1) and have a binding energy given by $\epsilon_d + U_{dd}(\Gamma) + \Delta_{d-sp}$, where ϵ_d is the energy required for removing a Cu $3d$ electron in the absence of correlation effects, $U_{dd}(\Gamma)$ is the Coulomb correlation energy for the particular symmetry Γ under consideration and Δ_{d-sp} is the $d-sp$ charge-transfer energy. Using values from Ref. 40 [$\epsilon_d = 3.1$ eV, $U_{dd}(^1G) = 9.2$ eV, and $\Delta_{d-sp} = 4.7$ eV], we obtain 17.0 eV, in reasonable agreement with the experimental value. The agreement can

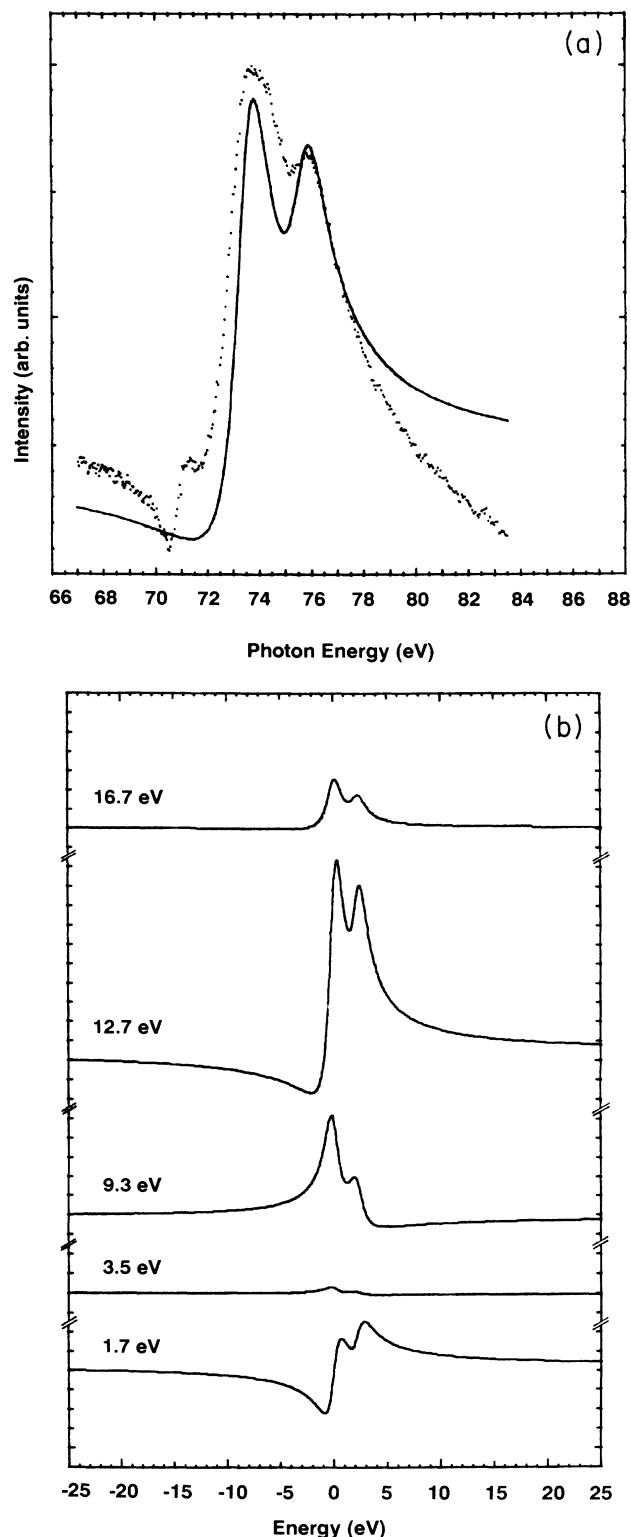


FIG. 4. (a) CIS spectrum measured at a binding energy of 12 eV (dotted line), compared with the results of cluster calculations (solid line). The data have been corrected for analyzer and monochromator transmission. Some contribution from the monochromator (mirror coating) may still be present at the Ni 3*p* edge (Ref. 13). (b) CIS curves calculated for some selected binding energies. For each curve, we have set the asymptotic value of the intensity to unity. One division on the vertical axis is 0.05.

probably be further improved by explicitly including the O 2*p*-Cu 4(*sp*) hybridization in the Hamiltonian.

V. CONCLUSION

Our calculation of the photoemission intensity for photon energies in the vicinity of the (3*p*→3*d*) resonance confirms some important points for the understanding of CuO. First, the resonance occurs mostly for final states that are overwhelmingly *d*⁸-like. The identification of these states with the peaks found between 8 and 13 eV binding energy^{1,3} is thus confirmed. To reproduce this spread, it is necessary to include the dependence of the Coulomb interaction upon the multiplet states in the calculations. Second, singlet final states play a much more important role than triplets in the resonance process, as was expected from the consideration of a simpler model.¹⁵ Also important is the much reduced resonance of the lowest binding energy peak, confirming its dominant *d*⁹ \underline{L} and *d*¹⁰ \underline{L}^2 character. These conclusions confirm the charge-transfer nature of the band gap in CuO. Finally, there is some indication that the transfer integral $t_{pd}(8)$ is larger than the transfer integral $t_{pd}(10)$. In addition, we have presented an explanation for the resonant photo-

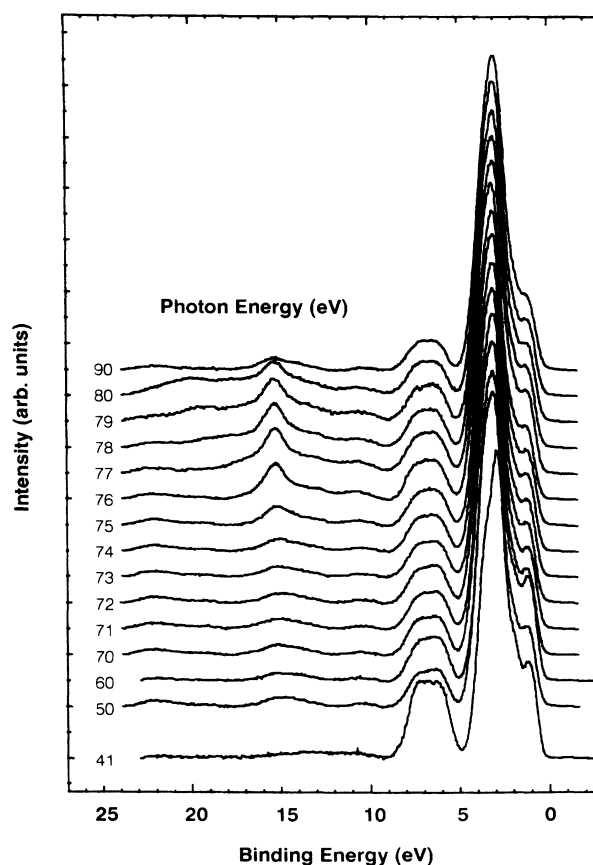


FIG. 5. Valence-band spectra of Cu₂O recorded around the Cu 3*p* threshold.

emission of Cu₂O which clearly shows the importance of O 2*p*–Cu 4(*sp*) hybridization.⁴¹

ACKNOWLEDGMENTS

We are grateful to François Grey for his assistance during the measurements and to A. Kotani and A. Fujimori for stimulating discussions. This work was supported by the Netherlands Foundation for Chemical

Research [Stichting Scheikundig Onderzoek in Nederland (SON)] and the Foundation for Fundamental Research on Matter [Stichting voor Fundamenteel Onderzoek der Materie (FOM)] with financial support from the Netherlands Organization for the Advancement of Pure Research (NWO) and by the Bundesminister für Forschung und Technologie (BMFT) under Grant No. 05 490 CAB.

- *Present address: Facultés Universitaires Notre Dame de la Paix, Laboratoire Interdisciplinaire de Spectroscopie Electronique, 61 rue de Bruxelles, B-5000 Namur, Belgium.
- ¹J. Ghijsen, L. H. Tjeng, J. van Elp, H. Eskes, J. Westerink, G. A. Sawatzky, and M. T. Czyzyk, *Phys. Rev. B* **38**, 11 322 (1988).
 - ²M. T. Czyzyk and R. a. de Groot (unpublished). The calculation method is described in H. V. Leuken, A. Lodder, M. T. Czyzyk, F. Springelkamp, and R. A. de Groot, *Phys. Rev. B* **41**, 5613 (1990).
 - ³H. Eskes, L. H. Tjeng, and G. A. Sawatzky, *Phys. Rev. B* **41**, 288 (1990).
 - ⁴J. Zaanen, G. A. Sawatzky, and J. W. Allen, *Phys. Rev. Lett.* **55**, 418 (1985); *J. Magn. Magn. Mater.* **54-67**, 607 (1986).
 - ⁵G. A. Sawatzky, in *Towards the Theoretical Understanding of High-T_c Superconductors*, edited by S. Lundqvist, E. Tosatti, M. P. Tosi, and Yu Lu (World Scientific, Singapore, 1988), p. 243.
 - ⁶H. Eskes, L. H. Tjeng, and G. A. Sawatzky, in *Mechanisms of High Temperature Superconductivity*, Vol. 11 of *Springer Series in Materials Sciences*, edited by H. Kamimura and A. Oshiyama (Springer, Berlin, 1989), p. 20.
 - ⁷L. H. Tjeng, H. Eskes, and G. A. Sawatzky, in *Strong Correlation and Superconductivity*, Vol. 89 of *Springer Series in Solid-State Sciences*, edited by H. Fukuyama, S. Maekawa, and A. P. Malozemoff (Springer, Berlin, 1989), p. 33.
 - ⁸G. A. Sawatzky, in *Earlier and Recent Aspects of Superconductivity*, Vol. 90 of *Springer Series in Material Sciences*, edited by J. G. Bednorz and K. A. Müller (Springer, Berlin, 1990), p. 345.
 - ⁹L. Ley, M. Taniguchi, J. Ghijsen, R. L. Johnson, and A. Fujimori, *Phys. Rev. B* **35**, 2839 (1987).
 - ¹⁰T. Ishii, M. Taniguchi, A. Kakizaki, K. Naito, H. Sugawara, and I. Nagakura, *Phys. Rev. B* **33**, 5664 (1986).
 - ¹¹M. L. Thuler, R. L. Benbow, and Z. Hurych, *Phys. Rev. B* **26**, 669 (1982).
 - ¹²C. Kunz, J. Schmidt-May, F. Senf, J. Voss, A. Flodström, R. Nyholm, and R. Stockbauer, *Surf. Sci.* **163**, 303 (1985).
 - ¹³S. Suga, *Phys. Scr.* **17**, 228 (1987).
 - ¹⁴P. Thiry, G. Rossi, Y. Petroff, A. Revcolevschi, and J. Jegoudez, *Europhys. Lett.* **5**, 55 (1988).
 - ¹⁵L. C. Davis, *Phys. Rev. B* **25**, 2912 (1982).
 - ¹⁶K. Okada and A. Kotani, *J. Phys. Soc. Jpn.* **58**, 1095 (1989).
 - ¹⁷R. L. Johnson and J. Reichardt, *Nucl. Instrum. Methods* **208**, 791 (1983).
 - ¹⁸S. Åsbrink and L.-J. Norrby, *Acta Crystallogr. Sec. B* **26**, 8 (1970).
 - ¹⁹A. K. McMahan, R. M. Martin, and S. Satpathy, *Phys. Rev. B* **38**, 6650 (1988).
 - ²⁰J. J. Yeh and I. Lindau, *At. Data Nucl. Data Tables* **32**, 1 (1985).
 - ²¹J. C. Slater, *Quantum Theory of Atomic Structure* (McGraw-Hill, New York, 1960), Vol. 1.
 - ²²U. Fano, *Phys. Rev.* **124**, 1866 (1961).
 - ²³L. C. Davis and L. A. Feldkamp, *Phys. Rev. B* **23**, 6239 (1981).
 - ²⁴E. C. McGuire (unpublished).
 - ²⁵Herman and Skillman, *Atomic Structure Calculations* (Prentice-Hall, Englewood Cliffs, 1963).
 - ²⁶L. C. Davis and L. A. Feldkamp, *Phys. Rev. A* **24**, 1862 (1981).
 - ²⁷L. C. Davis and L. A. Feldkamp, *Solid State Commun.* **19**, 413 (1976).
 - ²⁸L. I. Yin, I. Adler, T. Tsang, M. H. Chen, D. A. Ringers, and B. Crasemann, *Phys. Rev. A* **9**, 1070 (1974).
 - ²⁹We use the model matrix elements from Ref. 24. McGuire's tables give also values derived from a fit to ESCA data, which in our case are not significantly different.
 - ³⁰J. C. Fuggle and S. F. Alvarado, *Phys. Rev. A* **22**, 1615 (1980).
 - ³¹G. van der Laan, *Solid State Commun.* **42**, 165 (1982).
 - ³²J. Zaanen, C. Westra, and G. A. Sawatzky, *Phys. Rev. B* **33**, 8060 (1986).
 - ³³O. Gunnarsson, O. K. Andersen, O. Jepsen, and J. Zaanen, in *Core-Level Spectroscopy in Condensed Systems*, Vol. 81 of *Springer Series in Solid State Sciences*, edited by J. Kanamori and A. Kotani (Springer, Berlin, 1988), p. 82; *Phys. Rev. B* **39**, 1708 (1989).
 - ³⁴G. A. Sawatzky, in *Core-Level Spectroscopy in Condensed Systems*, Vol. 81 of *Springer Series in Solid-State Sciences*, edited by J. Kanamori and A. Kotani (Springer, Berlin, 1988), p. 99.
 - ³⁵H. Eskes and G. A. Sawatzky, *Phys. Rev. Lett.* **61**, 1415 (1988).
 - ³⁶F. C. Zhang and T. M. Rice, *Phys. Rev. B* **37**, 3759 (1988).
 - ³⁷J. Igarashi, *J. Phys. Soc. Jpn.* **54**, 2762 (1985).
 - ³⁸J. Igarashi and T. Nakano, *J. Phys. Soc. Jpn.* **55**, 1384 (1986).
 - ³⁹L. H. Tjeng, M. B. J. Meinders, J. van Elp, J. Ghijsen, G. A. Sawatzky, and R. L. Johnson, *Phys. Rev. B* **41**, 3190 (1990).
 - ⁴⁰L. H. Tjeng, J. van Elp, P. Kuiper, and G. A. Sawatzky (unpublished).
 - ⁴¹M. Grioni, M. T. Czyzyk, F. M. F. de Groot, J. C. Fuggle, and B. E. Watts, *Phys. Rev. B* **39**, 4886 (1989).